A Lower Limb Wearable Exosuit for Improved Sitting, Standing, and Walking Efficiency

Xiaohui Zhang[1], Enrica Tricomi[1], Xunju Ma[2], Manuela Gomez-Correa[3], Alessandro Ciaramella[4], Francesco Missiroli[1], Luka Mišković[5], Huimin Su[1], and Lorenzo Masia[6]

***Abstract*—Sitting, standing, and walking are fundamental activities crucial for maintaining independence in daily life. However, aging or lower limb injuries can impede these activities, posing obstacles to individuals' autonomy. In response to this challenge, we developed the LM-Ease, a compact and soft wearable robot designed to provide hip assistance. Its purpose is to aid users in carrying out essential daily activities such as sitting, standing, and walking. The LM-Ease features a fully-actuated tendon-driven system that seamlessly transitions between assistance actuation profiles tailored for sitting, standing, and walking movements. This device provides the user with gravity support during stand-to-sit, and offers hip extension assistance pulling force during sit-to-stand and walking. Our preliminary results show that with the LM-Ease, healthy young adults (n = 8) had significantly lower muscle activation: average reduction of 15.6% during stand-to-sit and 17.8% during sit-to-stand. Furthermore, with LM-Ease, participants demonstrated a 12.7% reduction in metabolic cost during ground walking. These evidences suggest that the LM-Ease holds potential in reducing muscular activation and energy expenditure during these fundamental daily activities. It could serve as a valuable tool for individuals seeking assistance in enhancing lower limb mobility, thereby bolstering their independence and overall quality of life.**

***Index Terms*—Wearable Robotics; Exosuits, Adaptive Lower Limb Assistance Control, Machine Learning.**

I. Introduction

IN our daily lives, the sequential process of "sitting-standing-walking" is a frequently repeated series of actions. Statistics indicate that healthy free-living adults perform approximately 60 repetitions of these actions on average each day [1]. The ability to independently execute these fundamental activities of daily living (ADLs) significantly contributes to personal autonomy and overall well-being. However, owing to the natural aging, congenital conditions, or acquired injuries, certain individuals may encounter difficulties in transitioning from stand-to-sit, sit-to-stand, or walking. These challenges stem from alterations in muscle composition and a decline in motor control [2], significantly curtailing their daily activities and reducing their independence [3].

Given the latest developments in the robotic field, there is a growing interest on technological products that can improve or enhance the capacity to execute fundamental ADLs. For instance, wearable lower limb assistive devices are gaining great attention as a potential response to this need and challenge [4]–[6]. These devices are intentionally designed to offer effective support to individuals with reduced muscle strength or lower limb impairments [7]–[9], potentially enhancing their muscle function and enabling them to perform ADLs tasks with increased independence and ease [10], [11].

Commonly found on the market, devices such as sit-stand lifts [12] and wearable powered exoskeletons [13], [14] are widely employed to facilitate sitting and standing transitions or walking assistance for frail users. These devices rely on rigid structures for support and mobility assistance, yet they are costly, power-intensive, and bulky, challenging their integration into daily life. In contrast to conventional rigid devices, wearable soft exosuits present customized lightweight and flexible designs suited for users, exhibiting reduced power consumption and lower costs [15]. Their working principles rely on human lower limb natural movements, acting in parallel to the user's muscles to provide the necessary assistance for accomplishing ADLs tasks [3].

Currently, research on soft wearable lower limb devices mainly focuses on assisting users in walking or running [10], [16]–[18], while research exploring the use of soft exosuits to assist with sitting and standing is notably lacking. Lee et al. [19] assessed a passive wearable soft exosuit utilizing elastic bands, demonstrating its potential to diminish the energy expenditure during users' sit-to-stand movements. Kulasekera et al. [20] proposed a low-profile vacuum actuator that utilizes a low-profile spring encased within a low-density polyethylene film to provide users with sit-to-stand assistance in a soft exosuit through vacuum actuation and passive recovery. Its effectiveness in reducing the user's muscle activation was verified. Schmidt et al. [21] demonstrated that the Myosuit, a commercially available wearable device utilizing a tendon-driven mechanism guided by a rigid knee joint and elastic bands at the hip, can also reduce the user's muscular activity when performing sitting and standing transitions.

In this study, we present the design and evaluation of a novel powered lower limb wearable hip exosuit, namely

[1]Xiaohui Zhang, Enrica Tricomi, Francesco Missiroli, and Huimin Su are with the Institut für Technische Informatik (ZITI), Heidelberg University, 69120 Heidelberg, Germany (Corresponding author: Xiaohui Zhang, e-mail: xiaohui.zhang@ziti.uni-heidelberg.de).

[2]Xunju Ma is with the School of Mechatronical Engineering, Beijing Institute of Technology, 100081 Beijing, China.

[3]Manuela Gomez-Correa is with the Medical Robotics and Biosignals Laboratory, Centro de Innovación y Desarrollo Tecnológico en Cómputo, Instituto Politécnico Nacional, 07340 Mexico City, Mexico.

[4]Alessandro Ciaramella is with the Institute of Mechanical Intelligence, Sant'Anna School of Advanced Studies, 56127 Pisa, Italia.

[5]Luka Mišković is with the Department of Automatics, Biocybernetics and Robotics, Jožef Stefan Institute, Jamova cesta 39, 1000 Ljubljana, Slovenia.

[6]Lorenzo Masia is with the Department of Computer Engineering, School of Computation, Information and Technology, Technical University of Munich (TUM), 80333 Munich, Germany.

LM-Ease (Lower-limb Movement Ease), designed to assist individuals in transitioning between sitting and standing, as well as facilitating walking. The hip joint, serving as a critical connection point between the trunk and lower limbs during movement, is a major player in generating and transmitting force [22], [23]. Given the pivotal role of the hip joint, the main goal of the LM-Ease exosuit is to provide effective hip assistance, empowering users to perform daily activities with enhanced ease and autonomy. The control system of the LM-Ease employs locomotion mode recognition and gait phase estimation algorithms to enhance synchronization between the user and the device. It is a tendon-driven system able to provide the users with stable anti-gravity support during transition from stand-to-sit, and hip extension assistance during transition from sit-to-stand and walking.

We hypothesize that wearing the LM-Ease exosuit would reduce users' muscle activity during the stand-to-sit and sit-to-stand transitions, as well as reduce metabolic cost of transport during walking. We also hypothesized that wearing the LM-Ease exosuit does not restrict users' natural movements. We have tested these hypotheses through experiments based on a comparison between performing sitting, standing, and walking actions with and without assistance from the LM-Ease device, monitoring and further comparatively analyzing the muscle activation, metabolic cost, and kinematics of eight participants.

The contributions of this study are primarily demonstrated in two aspects. Firstly, the newly designed soft lower limb assistive device, LM-Ease, has realized and verified for the first time that the soft-powered hip tendon-driven exosuit can provide gravitational support for users during the stand-to-sit transition, while also offering extension-assistive tension during sit-to-stand transition and walking. Secondly, this work includes a preliminary test on the feasibility of the LM-Ease in assisting users with sitting and walking, along with an analysis and evaluation of muscle activation, metabolic costs, and kinematics in participants. The practical implementation of this study is expected to advance the extensive application of textile-based soft assistive devices in the realm of wearable assistive technology. This, in effect, will encourage the seamless integration of assistive devices into everyday life, thereby improving autonomy in the performance of daily activities.

II. Exosuit Design

The fully-actuated LM-Ease exosuit (depicted in Fig. 1) has a weight of 3 kg and is specifically designed to provide hip support and extension assistance for the user.

The primary textile components of the LM-Ease exosuit comprise a waist belt and two thigh bandages. They are connected to each other by two artificial tendons (Anyasen Braided Waxed String, 2 mm diameter, Black, China), which are responsible for transmitting the assistive forces to the user by connecting the proximal (on the waist belt) and distal (on the bandages) anchor points (3D-printed) after passing through their respective head-end Bowden sheaths (Shimano SLR Mantel, 5 mm diameter, Japan).

The LM-Ease's control unit, actuators, and power supply are mounted on the back of the belt and represent most of the device's weight. The control unit primarily comprises a Nvidia Jetson (Nvidia Jetson Nano, USA) responsible for executing machine learning algorithm and an Arduino (Arduino MKR 1010 WiFi, Italy) that reads kinematic signals from the IMUs and manages the control of actuators. Additionally, the control unit includes a Feather (BLE, Feather nRF52 Bluefruit, Adafruit, USA) for receiving IMU signals transmitted via Bluetooth Low Energy (BLE) and a Can-bus extension board (Can-bus Shield V2.0, Seeed Studio, China) to facilitate communication between the controller and the motors.

The actuation system, situated at the base of the control unit, features two brushless motors (T-Motor, AK60-6, 24 V, 6:1 planetary gear-head reduction, CubeMars actuator, China) and a 3D-printed pulley with a diameter of 35mm was mounted on top of each motor.

On the lateral side of the thigh harnesses, two thigh IMU modules communicate with the control unit via the BLE protocol. Each IMU module is mainly comprised of a BNO055 (Bosch, Bno055, Germany) for measuring thigh kinematic signals and a Feather (BLE, Feather nRF52 Bluefruit, Adafruit, USA) for generating BLE signals for transmission. Another IMU is positioned atop the control unit at the back of the waist belt, connecting to the control unit via wires.

All electronic components draw power either directly or indirectly (via a 24V/12V to 5V 5A DC-DC buck power converter board) from a 14.8V battery (Tattu, 14.8V, 3700mAh, 45C, USA).

The times and procedure of one participant donning (1 minute 08 seconds) and doffing (56 seconds) the exosuit are demonstrated in the supplementary video material.

III. Methods

The embedded controller within this wearable LM-Ease exosuit is founded upon machine learning algorithms. It offers supplementary assistance to users in their daily activities (sitting, standing, and walking) by leveraging user's kinematic characteristics.

In recent years, methods of detecting motion patterns and identifying gait phases have been widely used in lower limb wearable devices to improve their assistive efficiency. For instance, various sensors such as cameras, IMUs, and EMGs, along with diverse machine learning algorithms [17], [24]–[27], have been employed for locomotion mode detection. Similarly, methods for gait phase estimation have been developed using adaptive oscillators [28], [29], phase portrait [30], [31], or machine learning techniques [32]. However, it remains a major challenge to design a control system that can use simple and easy to process sensors to accurately identify movement patterns while estimating gait phases in real-time.

Here, we focus on the real-time human-in-the-loop assistance utilizing only IMU sensors, as well as the construction of its internal locomotion pattern detection and gait phase recognition assistive models in terms of two parts: *Offline modelling* and *Real-time assistive control Framework*.

A. Offline Modelling

The locomotion mode detection and gait phase estimation models embedded in the controller were obtained offline using

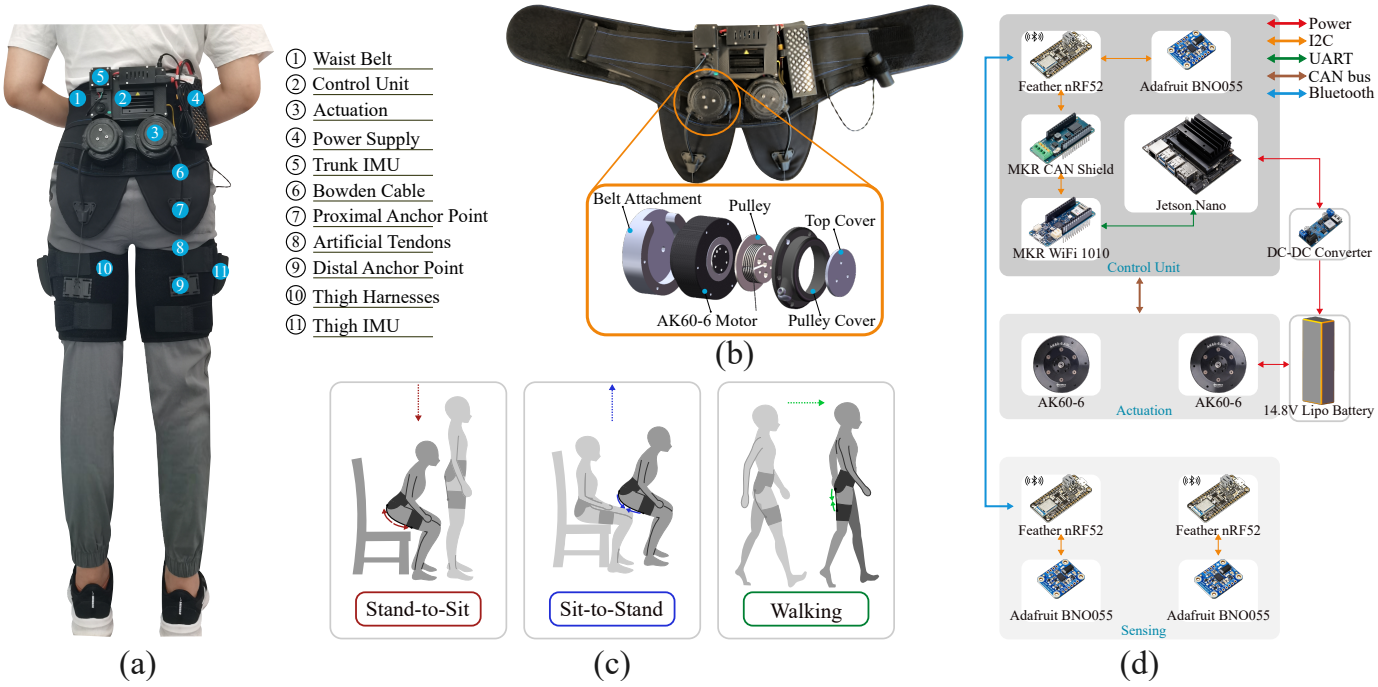

Fig. 1. **Design of the LM-Ease exosuit.** (a) The hip exosuit is a textile exomuscle consisting mainly of a waist belt that anchors the controller unit, the actuator unit, and the power supply, and a thigh bandage that anchors the sensor units. The assistive force is transmitted to the user by an artificial tendon connecting the proximal anchor point on the waist and the distal anchor point on the thigh under the action of a motor. (b) Mechanical design of the actuator unit for each leg. (c) The LM-Ease is designed to provide support for the user's stand-to-sit activity and to provide extension assistance for the user's sit-to-stand and walking activities. (d) Hardware components of the exosuit and communication protocols between hardware modules.

a purposeful experimental dataset derived from eight healthy participants.

The eight participants selected for the offline modelling experiment were free of disability. Prior to the initiation of the experiments, informed consent was obtained from each participant. All procedures adhered to the principles outlined in the Declaration of Helsinki, and this research received approval from the Ethical Committee of Heidelberg University under resolution S-313/2020.

1) Training dataset collection: Eight participants (six males and two females, age: 25.9±1.8 years, height: 1.78±0.10 m, weight: 72.4±12.8 kg, mean ± std) were enlisted to carry out the task of collecting the dataset used to train the LM-Ease's internal machine learning models. Each participant was instructed to perform two separate experimental sessions on these data collection-oriented lower-limb tasks:

a. Conducting ten rounds of transitions between sitting and standing, synchronized with an 8 beats per minute (bpm) metronome. In each round, participants were instructed to perform a transition from standing to sitting (stand-to-sit) upon hearing the metronome beat, followed by a transition from sitting to standing (sit-to-stand) upon hearing the next beat. The cycle continued for the duration of each round, with participants moving on to the next round at the sound of the following beat.
b. Continuous walking on level ground at a self-selected walking speed for 400 m, followed by standing still for one minute.

The kinematic data, comprising angles and angular velocities from the left leg, right leg, and trunk, was collected by three IMUs sampled at 100 Hz in the Matlab/Simulink R2021b environment (Mathwork, Massachusetts, USA). In order to correct for the angular drift of IMUs over prolonged usage of the device during walking, we additionally captured the real-time angle values for both the left and right legs after the application of a notch-peak filter (centered at 0 Hz). This strategy aims to eliminate hip angular drift measured by the IMUs during walking, retaining solely the relative angular change values centred on 0 degrees.

The collected data were used to train the locomotion mode recognition model and the gait phase estimation model.

2) Locomotion mode recognition model: The locomotion mode recognition model is used to differentiate and identify the user's sit-to-stand/stand-to-sit and walking patterns. The following procedure was performed offline for model training. ***Training data selection:*** For the purpose of improving the prediction accuracy of the model, we selectively choose training dataset based on the correlation and variability of kinematics across different locomotion modes, as well as past empirical knowledge, aiming to maximize model performance and generalization capability. The training dataset for locomotion mode recognition module incorporates eight distinct vectors. These vectors were derived from the participants' kinematic dataset (collected in Section III-A1) and encompassed the right leg thigh angle θ_{rt} and angular velocity v_{rt}, the left leg angle θ_{lt} and angular velocity v_{lt}, the trunk angle θ_{tr} and angular velocity v_{tr}, the sum of the angles of the right and left legs, computed by $\theta_{sum} = \theta_{rt} + \theta_{lt}$ and the sum of angular velocity, expressed as $v_{sum} = v_{rt} + v_{lt}$. Additionally, it is worth noting that our analysis of the kinematics from the IMUs revealed

an overlap in data features around the onset of the stand-to-sit transition, the end of the sit-to-stand transition, and the stand phase of walking gait. This overlap diminished the accuracy of the locomotion mode classification model. To improve the model's detection accuracy and better capture the variability of movement patterns, we included the sum of the angles θ_{sum} and velocities v_{sum} as additional training data features and set a threshold when labelling the sit-and-stand movement.

Training data labelling: The training dataset collected during sitting and standing task (described in Section III-A1-a) for locomotion mode recognition module, was divided into two distinct categories: one was labelled as "stand-to-sit" (from Point 1 to Point 2 in Fig. 2), representing the transition from standing to sitting, and the other was labelled as "sit-to-stand" (from Point 2 to Point 3 in Fig. 2), signifying the transition from sitting to standing. The remaining data, that are, the data between Point 3 and Point 1, were treated as a quiet standing state and were ignored and discarded. In each cycle of sitting and standing:

- point where $\theta_{sum} > 15°$ was regarded as the starting point (Point 1) for the stand-to-sit transition;
- positive peak point of the trunk angular velocity v_{tr} (Point 2) was marked as the endpoint for the stand-to-sit transition, and it also served as the starting point for sit-to-stand transition;
- point where $\theta_{sum} < 15°$ was considered as the endpoint (Point 3) for the sit-to-stand transition.

As for the walking and standing still task (described in Section III-A1-b), the dataset was manually labelled as "walking".

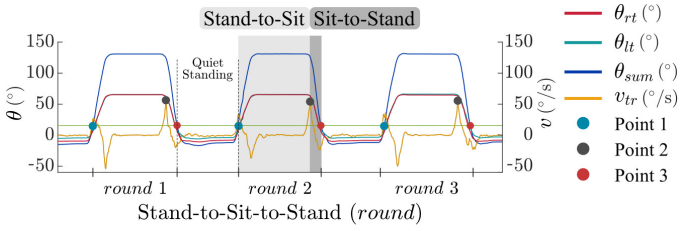

Fig. 2. **Sitting and standing labelling.** The colored lines record the kinematic signals of a typical participant during 3 rounds of "stand-to-sit-to-stand". Point 1 to Point 2 portion was labelled as "stand-to-sit" and Point 2 to Point 3 portion was labelled as "sit-to-stand".

Feature extraction: we implemented a sliding window technique to extract features and corresponding labels of the dataset that is ultimately used to train the model. As shown in Fig. 3, taking the current position of the sliding window for feature extraction of sitting and standing as an example, the current sliding window spans a total of eight selected vectors, and each vector comprises 30 sampled data points (i.e. 300 ms sampled at 100 Hz). For each vector, we derive six values from these 30 sampled data points: first, last, maximum, minimum, mean, and standard deviation (std) values. At the end, by combining the six extracted features from each of the eight vectors, a total of 48 features are formed to represent the sample data at the current window position. The last value of the label channel corresponding to the current window position is regarded as the label of this sample data.

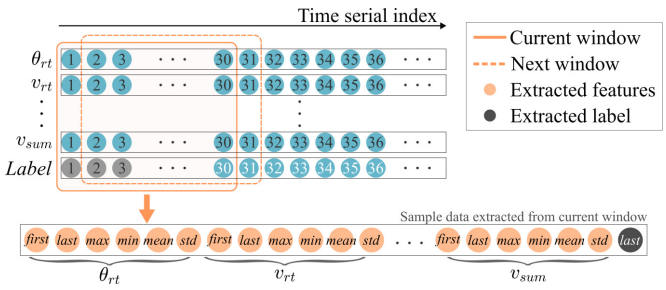

Fig. 3. **Feature extraction technique.** Six features (orange balls) for each vector (blue balls) in the current window (solid orange box) are extracted.

Modelling: Locomotion mode recognition was achieved through a random forest classification algorithm [33], [34]. We developed this algorithm in a MATLAB/Simulink 2021b environment (MathWorks, Massachusetts, USA), utilizing the *fitcensemble* function from the Statistics and Machine Learning Toolbox. The model employs decision trees as its base learner with the number of maximum splits set to 128 and the number of decision trees set to 10 and the final prediction of the model is determined by the majority vote of the base decision trees. Upon completing the training process, the model exhibits an approximate misclassification rate (MCR) of 0.15% during 10-fold cross-validation.

3) Gait phase estimation model: The function of the gait phase estimation model is to estimate the user's gait phase based on the user's leg state. The following steps were performed to train the model.

Training data selection: The training dataset collected during 400 m walking task (described in Section III-A1-b) for the gait phase estimation module, consists of two distinct vectors within the participants dataset: the notch-peak filtered right leg angle $\theta_{rt_{npf}}$ and the angular velocity of the right leg v_{rt}, respectively.

Training data labelling: In Fig. 4, an example of five gait cycles is used to elucidate the process of generating the target output signal for the gait phase estimation model. To begin, the maximum (blue dots) and minimum (black dots) points of $\theta_{rt_{npf}}$ (blue line) were detected, signifying the maximum flexion point (MFP) and maximum extension point (MEP) during walking, respectively. Subsequently, the gait phase vector T (i.e., the generated gait phase, black dotted line) was created by creating linearly spaced values in the range $[-\pi\ 0]$ between MFP and MEP, and values in the range $[0\ \pi]$ between MEP and MFP. Ultimately, the model computes its target output in the form of $Y = sin(T+\tau)$ (red line) to avoid the discontinuity of T in between gait cycles (i.e., from π of the last stride to $-\pi$ of new stride). Here, $\tau \in [0, \pi]$ represents the time-delay compensation parameter, which can be adjusted to suit different device gait configurations or delays according to the designer's requirements [17]. In our study, we set $\tau = 0$.

Feature extraction: Using the same technique as the sliding window based feature extraction described in *Locomotion mode recognition model* (Section III-A2), we constructed 12 features for the gait phase estimation model. These 12 features consist of six metrics (first, last, maximum, minimum, mean,

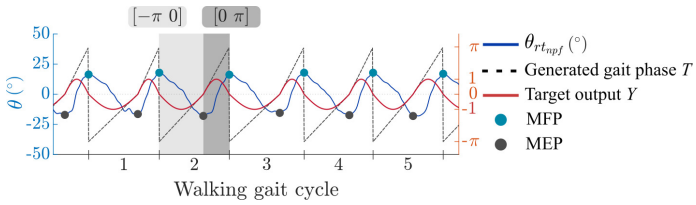

Fig. 4. **Gait phase labelling.** The collected gait signal $\theta_{rt_{npf}}$ is marked by the maximum flexion point (MFP) and maximum extension point (MEP), thereby generating the target output Y for training the gait phase estimation model.

and std) extracted from each of the two vectors ($\theta_{rt_{npf}}$ and v_{rt}).

Modelling: The gait phase estimation model employs the random forest regression algorithm [33], [34], which was developed using the *fitrensemble* function from the Statistics and Machine Learning Toolbox in a MATLAB/Simulink 2021b environment. The model consists of 30 decision trees, each allowing up to 1024 splits, with the final prediction determined as the average of the base decision trees' predictions. In 10-fold cross-validation, the final model attained a mean square error (MSE) of 0.81%.

B. Real-time Assistive Control Framework

Once the offline modelling is in place, the user can benefit from assistance in real-time provided by the Real-time Assistive Controller.

The operational mechanism of the LM-Ease exosuit for delivering real-time assistance to users is shown in Fig. 5.

When the user wears the LM-Ease exosuit, IMU sensors located on the left and right thighs as well as the trunk capture the user's kinematic signals. Subsequently, the machine learning models extract the kinematic features in real-time from the acquired kinematic signals, generating a prediction every 10 ms (We utilized the same online approach for feature extraction as we did offline, where each sliding window consisted of 30 real-time samples of data running at a frequency of 100 Hz. The sliding window moves forward by one sample with each new sampling, overlapping with the previous window by 29 samples.). These features are input to the locomotion mode recognition model (detailed in Section III-A2) within the controller to detect the user's motion state, such as detecting whether the user is in sit-and-stand transitions or engaged in ambulation. Simultaneously, the gait phase model (detailed in Section III-A3) predicts the user's current gait phase based on the extracted kinematic features.

Based on the prediction results of the models, a motor trajectory generator produces a customized reference profile suitable for the actuator's motion. Finally, an LP-filtered proportional controller directs the motor rotation to supply assistive force to the user by converting the error between the actual motor position and the reference motor position into motor angular velocity, with the following transfer function:

$$H_p(s) = \frac{K_p}{1 + K_d \cdot s} \tag{1}$$

where the coefficients $K_p = 8$ and $K_d = 0.06$ were fixed throughout the study, having been experimentally determined to optimize the tracking performance.

The alignment between the motor reference motion profile and the user's leg position during the gait phase was established and evaluated through iterative testing by a representative wearer. The trajectory generator R_{traj} under different locomotion modes (taking the right leg as an example) was customized as follows based on the motor configuration and pulley diameter in this study. However, it is worth to note that for different hardware configurations, the correlation coefficients in R_{traj} for each mode need to be adjusted to match the specific hardware.

a. *Stand-to-Sit:* When the controller detects that the user is in stand-to-sit transition mode, the right leg motor (as shown in Fig. 5(a)) rotates clockwise in proportion to the increasing hip flexion angle of the right leg ($R_{traj} = 1.5 * \theta_{rt}$). This rotation loosens the artificial tendon, providing continuous supportive force to the user during the stand-to-sit transition.
b. *Sitting:* During the stand-to-sit mode, the trajectory generator R_{traj} will automatically switch to "sitting" mode after three seconds until the controller detects sit-to-stand mode. In sitting mode, the motor will quickly relax the tendon based on the current right leg angle ($R_{traj} = 5 * \theta_{rt}$). This ensures that the exosuit is transparent and does not restrict the user's sitting position, thus enhancing comfort.
c. *Sit-to-Stand:* When the controller detects that the user is in sit-to-stand transition mode, the motor assisting the right leg rotates counterclockwise to quickly tighten the tendon, providing tension to assist the user in standing up. Since the changes of the right leg hip angle was insufficient to meet our required level of assistive force during sit-to-stand transition, we decided to adjust the motor reference profile in this mode based on the velocity of the right leg angle ($R_{traj} = 2 * v_{rt}$).
d. *Walking:* The motor reference profile in walking mode is set according to the predicted output of the gait phase estimation model ($R_{traj} = k * Y$, where $k \in [1, 5]$ can be adjusted appropriately according to the user's assistance requirements).

To ensure smooth transitions and prevent abrupt movements of the motor when switching between different modes, a second-order low-pass filter with a cutoff frequency of 4.8 Hz is employed to smooth the final motor reference profile.

The orientation of the motors and IMUs for the LM-Ease exosuit is defined as follows: as depicted in Fig. 5(a), the motor assisting the left leg tightens (positive direction) with clockwise rotation and releases (negative direction) with counterclockwise rotation. Conversely, the motor assisting the right leg tightens with counterclockwise rotation (+) and releases with clockwise rotation (−); Regarding the trunk IMU, the starting angle is 0° when the participants were standing still. A forward tilt of the trunk is measured in the negative direction, while a backward tilt is measured in the positive direction. For the thigh IMUs, similarly, the initial angle is 0° when standing

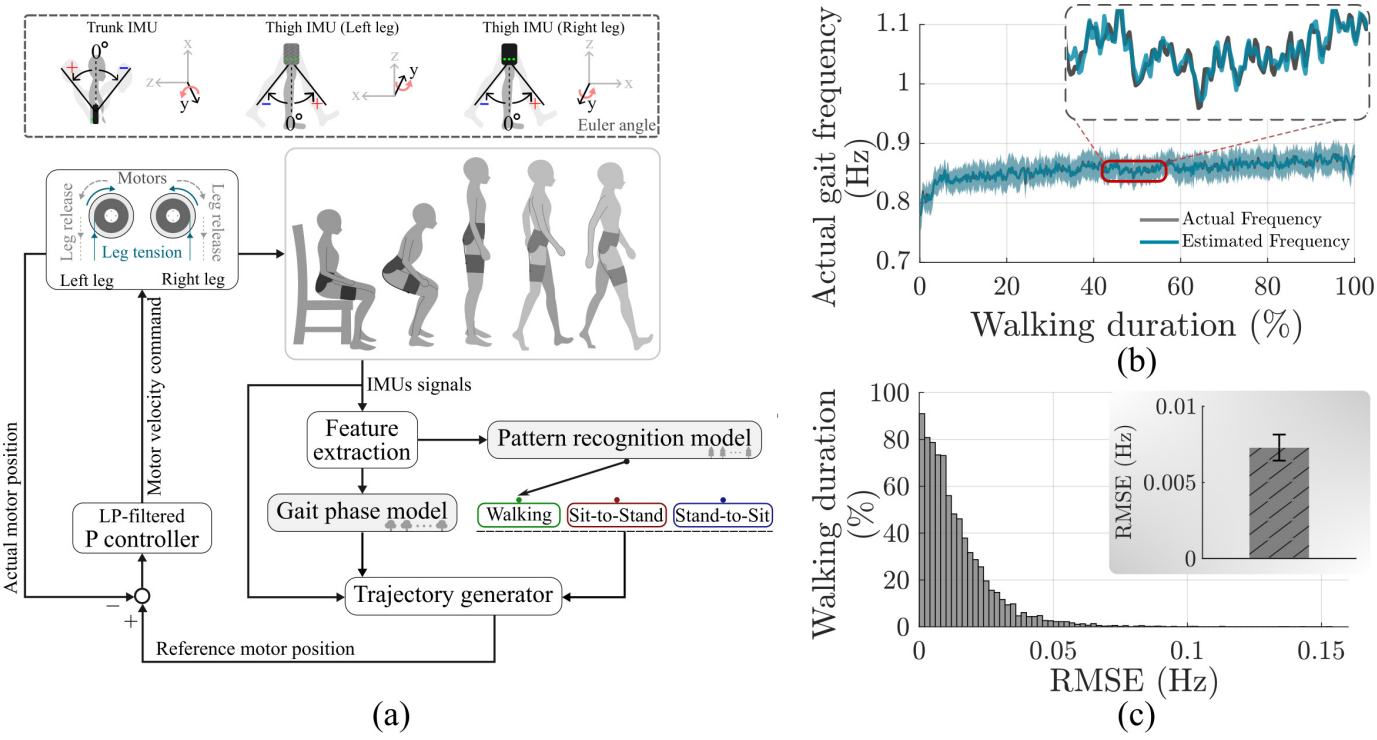

Fig. 5. **Assistance controller framework and performance.** (a) Controller framework and sketch of the orientation of the motors and IMUs. The real-time operational framework of the controller operates as follows: Initially, the IMU sensors on the device capture the wearer's kinematic data. Subsequently, through online feature extraction, the machine learning algorithm performs pattern recognition and gait phase estimation, analyzing the user's current motion state to generate an assistive trajectory. Finally, the motors are driven to align with this trajectory, providing supportive force for human movement. (b) Actual gait frequency (grey) recorded by IMU sensors and estimated gait frequency (blue) from the gait estimation model in the *ExoOn* condition throughout the walking duration and its partial enlarged view across participants. (c) The performance of gait phase estimation is illustrated by the root mean square error (RMSE) distribution histogram between actual and estimated gait frequencies and the average of RMSE across steps and participants during the entire walking experiment.

still. Hip flexion is measured as a positive direction for angle and angular velocity, whereas hip extension is measured as a negative direction. For both the trunk and thigh IMUs, we measure the euler angles and angular velocities along the y-axis using the BNO055 IMU sensors, while the measurements along the x-axis and z-axis are not utilized.

IV. Experiment

A. Participants

Eight participants (five males and three females, age: 27.5 $\pm$ 2.5 years, height: 1.74 $\pm$ 0.11 m, and weight: 62.5 $\pm$ 10.2 kg, mean $\pm$ std) without impairments were recruited.

The eight participants involved in the LM-Ease effectiveness validation experiment were in good physical health, and none had a history of musculoskeletal or neurological disorders. Informed consent was provided to participants before the start of the experiment, and all procedures adhered to the ethical standards outlined in the Declaration of Helsinki. Furthermore, approval for this experiment was also granted by the Ethical Committee of Heidelberg University under resolution S-313/2020.

B. Experiment Design and Protocol

The primary objective of this experiment was to assess the efficacy of the proposed lower limb wearable assistive device LM-Ease in facilitating daily activities of sitting, standing, and walking. The study was structured as a controlled trial aimed at investigating the impact of the device on users' muscle activity, energy consumption, and kinematic characteristics during stand-to-sit/sit-to-stand transitions and walking.

The experiment involved two conditions: one in which the participant did not receive any assistive force (*ExoOff*), and the other in which the participant received assistive forces generated by the LM-Ease (*ExoOn*). The sequence of experimental conditions was randomized for each participant, and between each condition, participants were instructed to take a minimum rest period of 20 minutes to minimize the impact of fatigue on the study results.

A wireless surface electromyography (EMG) system from Delsys (Trigno, Natick MA, USA) was utilized to assess the impact of the device on muscular effort. A portable gas analyzer (K5, COSMED, Rome, Italy) was employed to evaluate the metabolic cost during the task.

1) Experimental Setup: Prior to the initiation of the experimental task, the electrodes of the EMG system were positioned on the participant's body in accordance with SENIAM guidelines [35]. Muscle activity was recorded for three muscles contributing to the sitting and standing movements: Vastus Lateralis (VL), Rectus Femoris (RF), and Gluteus Maximus (GM). However, Gluteus Maximus data were omitted from subsequent offline analysis due to interference caused by the

device operation on the probe application point.

Afterwards, participants wore the respirometry equipment and underwent a four minutes data collection phase while maintaining a stationary standing position. The average metabolic value derived from the final two minutes served as the baseline P_0, to be subtracted from the ensuing active metabolic costs during data post-processing. This procedure was implemented to isolate and identify potential errors associated with the calibration of the metabolic gas exchange measurement device.

After completing the above operations and taking a short break, the participant was instructed to maintain a stationary standing position for 10 seconds after the device was powered on. During this period, the controller resets the initial positions of the IMUs and motors to zero, and the artificial tendon is pre-tensioned until the motor torque reading reaches 0.2 Nm. This procedure aims to minimize the influence of variations in participants' body sizes or initial postures on the device's initial positioning, thereby ensuring that the assistive torque is accurately delivered.

2) Experimental Protocol: Participants were instructed to execute an identical validation experimental task in both the *ExoOff* and *ExoOn* conditions. Each experimental task was subdivided into the following three distinct parts.

In the first part of the experiment (Exp: Part 1), participants were tasked with completing 20 rounds of transitioning between sit-to-stand and stand-to-sit, aligning their actions with an 8 bpm rhythm set by a sound metronome.

The second part of the experiment (Exp: Part 2) focused on assessing the efficacy of assistive forces from the exosuit during the user's walking activity. Participants were requested to engage in continuous walking with a self-selected walking speed over a distance of 680 m on a level surface (10 loops, each 68 m in circumference).

The third part of the experiment (Exp: Part 3) aimed to assess the reliability of the locomotion mode recognition algorithm integrated into the controller during continuous transitions between walking, sitting, and standing modes. Participants were instructed to perform one sit-to-stand and stand-to-sit transitions every 5 m of walking, repeated ten times in succession.

3) Data Acquisition: The EMG data were collected using a DAQ board (Quanser QPIDe, Ontario, Canada) at a sampling rate of 1 kHz. Metabolic data were recorded using COSMED OMNIA v1.6 in a Breath-by-Breath mode. The absence of a portable station for muscle activity collection hindered our ability to assess muscle activation during the walking experiment (Exp: Part 2). Consequently, the results from the first part of the experiments encompassed both EMG and metabolic measurements, while the analysis of the walking experiment predominantly concentrated on the metabolic cost of walking. Kinematic data, in conjunction with real-time controller data, were captured at a frequency of 100 Hz within the Matlab/Simulink R2021b environment running in the Nvidia Jetson installed on the exosuit.

C. Data Analysis and Statistics

Data post-processing was implemented in MATLAB R2021b. We analysed the assistive efficacy of the LM-Ease for the user in terms of muscle activation, metabolic saving, and user kinematics.

1) Controller Performance: The performance assessment of the designed locomotion mode recognition algorithm encompassed examining the algorithm's detection accuracy of participants' sitting, standing, and walking movements. Specifically, the evaluation comprised the sitting and standing detection accuracy for the 20 consecutive stand-to-sit-to-stand (sit-and-stand) cycles in the first part of the experiment (Exp: Part 1), the walking mode detection rate for consecutive walking in Exp: Part 2, and the sitting, standing, and walking continuous transitions in Exp: Part 3. The real-time predicted locomotion mode throughout the experiment for a representative participant are also shown in the results section.

Furthermore, an evaluation was conducted to verify the accuracy of gait phase estimation model. This entailed an analysis and comparison between the model's estimated gait frequency and the actual gait frequency as recorded by the IMUs during the participants' walking experiment portion. Subsequent to this, we computed the root mean square error (RMSE) between the actual and estimated gait frequencies to examine the estimation performance.

2) Muscular Activity: To assess the impact of LM-Ease exosuit on users' muscle activity during sitting and standing, the raw EMG signals were first band-pass filtered (20-400 Hz, 4^{th} order Butterworth), then sequentially full-wave rectified and low-pass filtered (6 Hz, 4^{th} order Butterworth) to derive the EMG envelope. Normalization of the signals was performed based on each subject's maximum voluntary contraction (MVC) during the experiment. The root mean square (RMS) value of the EMG envelope of stand-to-sit and sit-to-stand procedures across participants was used as an indicator of muscle activity assessment.

3) Cost of Transport: The metabolic power of participants in *ExoOff* and *ExoOn* conditions were calculated using the Péronnet and Massicotte equation [36]:

$$P = 16.89V_{O_2} + 4.84V_{CO_2} \tag{2}$$

which is based on the volume of oxygen V_{O_2} and carbon dioxide V_{CO_2} exchanged per breath during movements. The derived metabolic power P, adjusted by subtracting the average metabolic cost of quiet standing P_0, were then standardized based on the participant's body weight w and average movement speed v to obtain results in terms of cost of transport C.

$$C = \frac{P - P_0}{w * v} \tag{3}$$

The v for walking was calculated by dividing the total distance (680 m) walked by the total walking time. For sit-and-stand cycles, v represents the participant's average angular velocity over 20 sitting and standing cycles. This normalization facilitated comparison across participants and experimental conditions.

4) Kinematic Assessment: In order to evaluate the physiological impact of LM-Ease exosuit assistance on participants' natural sitting, standing, and walking movements, we analyzed changes in participants' range of motion (ROM) and movement velocity in *ExoOff* and *ExoOn* conditions. Quantitative kinematic results were presented by comparing the positive and negative peak values of ROM and movement velocity. This analysis was conducted after low-pass filtering (10 Hz, 4^{th} order Butterworth) the raw kinematic signal and then segmenting into sit-and-stand rounds and walking gait cycles.

The corresponding motor torque during each sit-and-stand movement and each gait cycle during walking, normalized by individuals' body weight, is also provided as an indication of the provided assistance by the device.

5) Statistical Analysis: The normality of the data distribution was assessed using the Shapiro-Wilk test at a significance level of $\alpha = 0.05$. Subsequently, a linear mixed-effects model employing the least squares regression method was utilized for the statistical analysis. The model encompassed the "condition" (*ExoOff*, *ExoOn*), represented as dummy-encoded categorical fixed-effect explanatory variables. The term "participant" (n = 8) was incorporated into the model as a random-effect variable.

V. Results

All participants (n = 8) completed the experimental trial successfully without experiencing any injuries or falls.

Results are expressed as mean ± sem (standard error of the mean), unless specified otherwise.

A. Accurate locomotion mode recognition and gait detection.

The locomotion mode recognition model was able to accurately and reliably detect the sitting, standing, and walking states of the different participants with a 100% detection rate, both in the 20-rounds sit-and-stand portion (Exp: Part 1), walking portion (Exp: Part 2), and the dynamic stand-sit-stand-walking switching portion (Exp: Part 3) of the experiment. Figure 6 shows the real-time predicted locomotion mode throughout the experiment for a representative participant.

Figure 5(b) and (c) present the evaluation results of the gait detection model. As shown in the curves of the actual gait frequency recorded by the IMUs and the gait frequency estimated by the model in Fig. 5(b), the gait estimation model demonstrates high accuracy in estimating gait frequency (referring to stride frequency across right and left legs). The average actual gait frequency across participants recorded by IMUs in the *ExoOn* condition throughout the walking duration was 0.86 ± 0.21 Hz, while the RMSE (shown in Fig. 5(c)) between the actual and estimated gait frequencies is $(7.3 \pm 0.86) \times 10^{-3}$ Hz (≈ 0.86% of the average actual gait frequency) on average across steps and participants. The RMSE distribution is also displayed in Fig. 5(c).

B. Muscle activity decreased when using LM-Ease.

Figure 7 depicts the effect of our lower limb assistive device on participants' muscular activity during sitting and standing

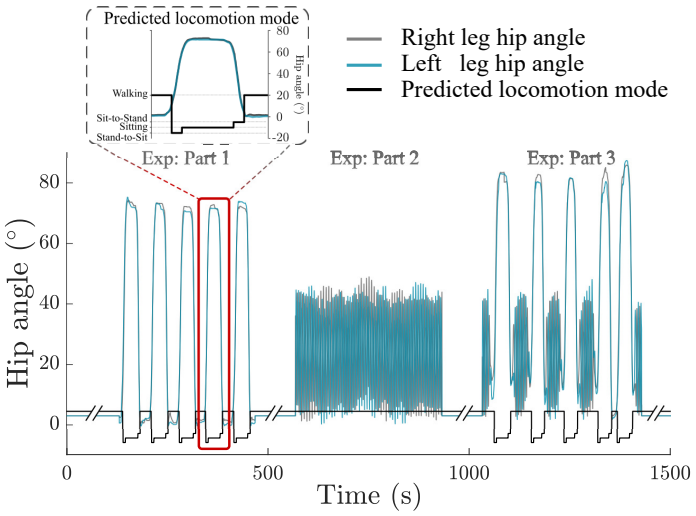

Fig. 6. **Real-time predicted locomotion mode throughout the experiment for a representative participant.** The grey line represents the right leg hip angle, the blue line represents the left leg hip angle, and the black line indicates the predicted locomotion mode.

movements, specifically targeting the muscles engaged in the stand-to-sit and sit-to-stand processes, Vastus Lateralis (VL) and Rectus Femoris (RF), respectively. Figure 7(a) and (b) present the average EMG envelope of muscle activation and the corresponding average normalized root mean square (RMS) values across 20 repetitions of the stand-to-sit and sit-to-stand for eight participants.

The findings revealed a significant decrease of 15.6%MVC (p=0.02) of the average RMS value of the VL muscle activation among participants during the stand-to-sit transition when the LM-Ease provided supportive force. Specifically, the mean values recorded were 28.3 ± 1.6%MVC for *ExoOff* and 23.9 ± 2.3%MVC for *ExoOn*. Similarly, during the sit-to-stand transition, when the device supplied assistive pulling force, the participants' VL muscle activation average RMS value significantly decreased by 17.8%MVC (p=0.002), reaching 38.6 ± 2.0%MVC with *ExoOff* and 31.7 ± 1.6%MVC with *ExoOn*, respectively.

Additionally, participants experienced a significant decrease in RF muscle activation by 11.4%MVC (p=0.02) during the sit-to-stand under the *ExoOn* condition, with values of 26.6 ± 4.0%MVC for *ExoOff* and 23.6 ± 2.7%MVC for *ExoOn*. However, the impact of exosuit assistance on lowering RF activity during the stand-to-sit transition has not been significantly shown.

C. Metabolic cost of transport was reduced with the LM-Ease.

The metabolic cost of transport, displayed in Fig. 8, details the participants' energy expenditure from 3 minutes post-initiation of the sit-and-stand and walking portion of the experiment, respectively.

In comparison to the *ExoOff* condition, participants demonstrated a significant 12.7% reduction in the average metabolic cost of walking with the aid of the device-assisted force, corresponding to 2.4 ± 0.1 $Jkg^{-1}m^{-1}$ for *ExoOff* and 2.1

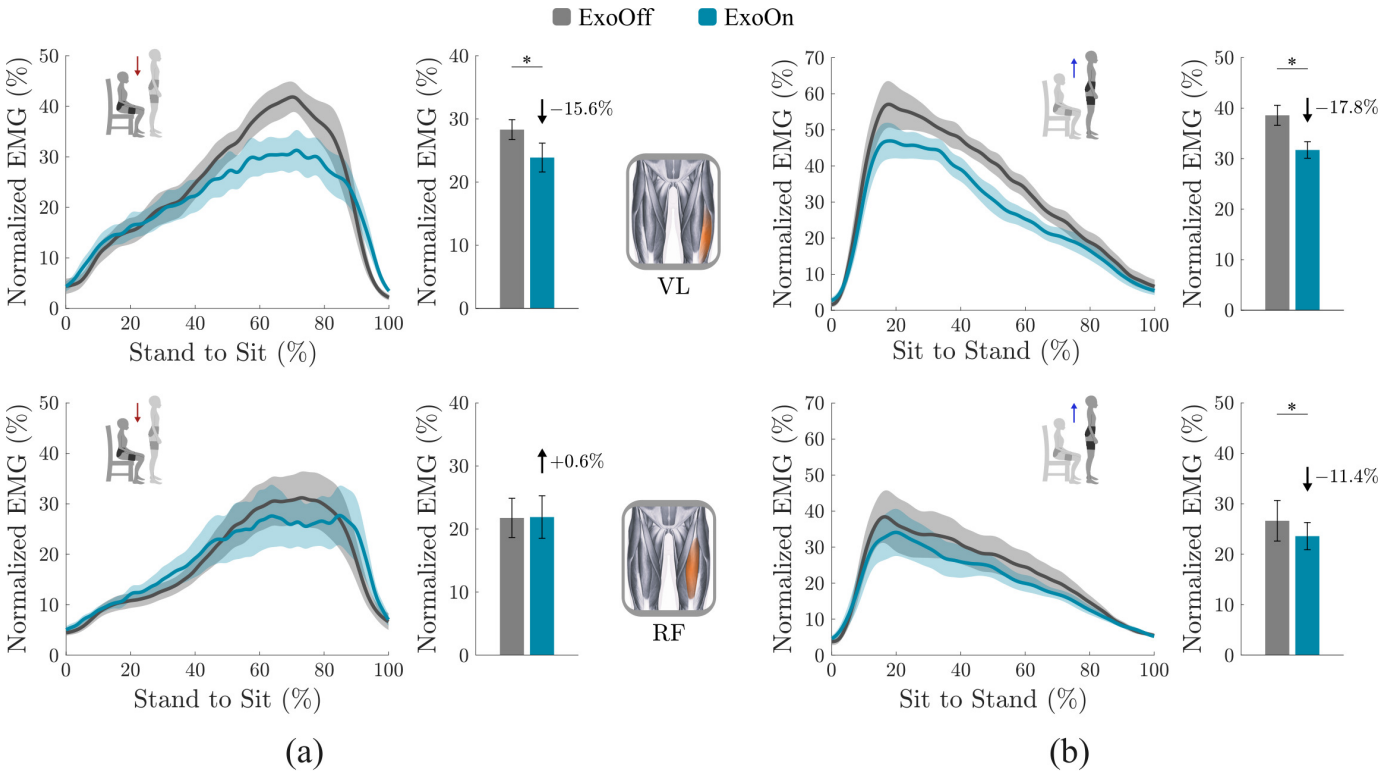

Fig. 7. **Effects on muscular activity.** EMG envelopes (curves) and RMS (bars) of Vastus Lateralis (VL) and Rectus Femoris (RF) during (a) stand-to-sit and (b) sit-to-stand transitions averaged across participants in *ExoOff* (grey) and *ExoOn* (blue) conditions. Asterisks * indicate statistically significant differences.

$\pm$ 0.1 Jkg^{-1}m^{-1} for the *ExoOn*, respectively. As for sit-and-stand movements, the energy loss results showed a slight but insignificant downward trend of 1.7% when wearing the LM-Ease.

Notably, the average walking speed used for normalizing net metabolic power increased by 5.8% with the LM-Ease, measuring 1.03 $\pm$ 0.05 m/s for *ExoOff* and 1.08 $\pm$ 0.03 m/s for *ExoOn* (depicted in Fig. 8(b)). The mean angular velocity during sit-and-stand cycles (averaged between stand-to-sit and sit-to-stand transitions) decreased by 2.7% (shown in Fig. 8(d)). However, neither walking speed nor sit-and-stand speed for energy normalization showed statistically significant differences compared to the *ExoOff* condition.

D. Unrestricted natural kinematic for the User.

The support and assistance provided by the lower limb LM-Ease device did not impose limitations on the range of motion of the participants, as shown in Fig. 9(a) and (c). This finding remains consistent for transitions from stand-to-sit, sit-to-stand, as well as during walking.

Sit-and-Stand: Specifically, during the sitting and standing experiment, as participants executed stand-to-sit transition, the LM-Ease exosuit provided gravity support force to the users. As a result, owing to the resistance provided by the exosuit, a noticeable decrease ($p<0.001$) in the participant's movements velocity was evident during the stand-to-sit transition, bringing to a 40.5% reduction of the positive peak velocity during voluntary sitting (velocity peaks of 67.7 $\pm$ 8.3°/s for *ExoOff* and 40.2 $\pm$ 4.2°/s for *ExoOn*). Consequently, the average total time for stand-to-sit transition across participants significantly ($p<0.001$) increased from 2.1 $\pm$ 0.2s to 3.5 $\pm$ 0.3s.

Moreover, as participants executed sit-to-stand transition, the lower limb exosuit provides assistance pulling force to the users. The participants' negative peak velocity of standing up significantly increased from -78.8 ± 7.4°/s in *ExoOff* to -89.4 ± 6.0°/s in *ExoOn* ($p=0.04$).

In the transition from stand-to-sit, the peak torque generated by the exosuit motor was 0.044 $\pm$ 0.008 Nm/kg across participants (depicted in Fig. 9(b)), whereas for sit-to-stand transition, the maximum motor torque was 0.055 $\pm$ 0.008 Nm/kg.

Walking: In comparison to *ExoOff*, the LM-Ease resulted in a notable 8.4% increase in the mean range of motion ($p<0.001$), with the mean maximum extension angle showing a significant increase of 4.5° ($p=0.003$): [-9.5 ± 1.3°, 29.2 ± 1.1°] for *ExoOff* and [-14.0 ± 0.9°, 27.9 ± 1.3°] for *ExoOn*, respectively. Additionally, the average velocity range exhibited a significant amplification of 12.3% ($p=0.001$): [-86.9 ± 5.5°/s, 158.2 ± 10.3°/s] for *ExoOff* and [-102.7 ± 5.5°/s, 172.6 ± 11.8°/s] for *ExoOn*.

The average peak motor torque generated by the LM-Ease exosuit across participants during the walking experiment (depicted in Fig. 9(d)) was 0.021 $\pm$ 0.003 Nm/kg.

VI. Discussion

Sitting, standing, and walking are the most common functional activities we perform in our daily life. With the aging process, being able to sit down smoothly and get up quickly

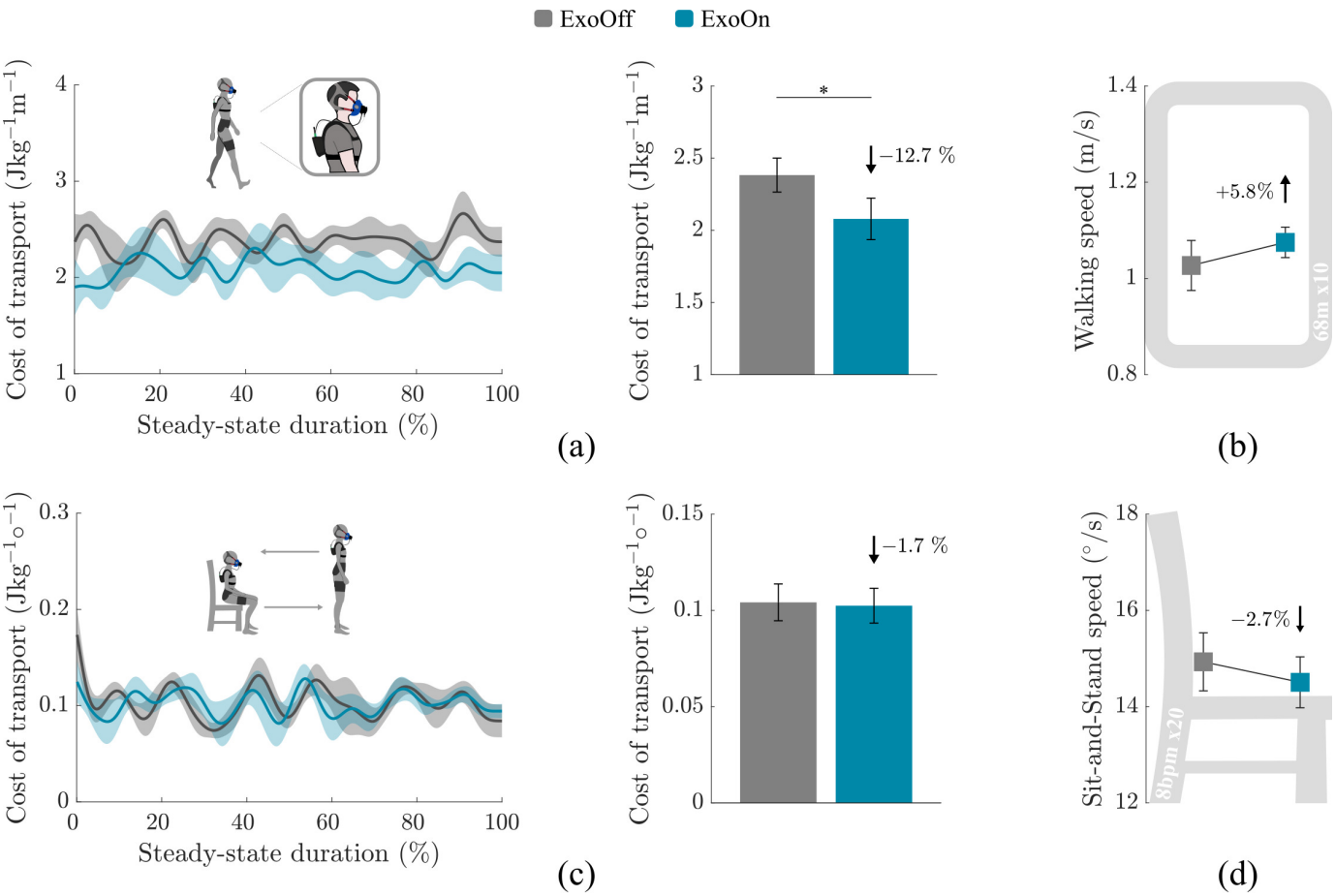

Fig. 8. **Effects on metabolic cost of transport.** (a,c) The metabolic cost curves and mean values for steady-state walking transport and sit-and-stand activity under *ExoOff* (grey) and *ExoOn* (blue) conditions. (b,d) The effects of the LM-Ease exosuit on users' walking speed and sit-and-stand speed. Asterisks * indicate statistically significant differences.

from a chair, as well as to maintain an active lifestyle, become more and more challenging. To keep performing these actions in an efficient way, we have designed a wearable lower limb exosuit−LM-Ease, aimed at assisting individuals in both stand-to-sit/sit-to-stand transitions and walking. This exosuit relies on a tendon-driven mechanism to alleviate muscular effort during the transitions between sitting and standing, while concurrently reducing energy expenditure during ambulation.

In contrast to our earlier efforts [17], [29], [37] aimed at assisting hip flexion while walking, the newly designed LM-Ease is intended to aid hip extension, which proves more meaningful when performing sitting/standing task [22], [38]. Additionally, we implemented an intuitive controller being able to discriminate in real-time among sitting/standing/walking actions and adapt the assistance profile accordingly. It is important to note that the significant variations in machine learning methods used for locomotion mode recognition and gait phase estimation across previous studies, along with different training data resources [32], [39], limit direct performance comparisons with our approach. Major differences stem from varying device types, sensor configurations, and research objectives, resulting in diverse approaches to training data selection, data labeling, and feature extraction. Despite these differences, we believe that our control methodology, based on a simple sensor configuration, can serve as a valuable reference for various lower limb wearable assistive devices in the context of the current literature.

As assessing the effectiveness of an assistive device commonly involves monitoring the user's muscle activation [3], [29], [40]. Here, we monitored the muscle activity of the Vastus Lateralis (VL) and Rectus Femoris (RF) muscles involved in both stand-to-sit and sit-to-stand transitions. As shown in Fig. 7, participants showed a downward trend in muscle activation during sitting and standing transition with the assistance of the LM-Ease. Specifically, for the VL muscle, compared to the unassisted condition, the muscle activation significantly decreased by 15.6%MVC for the stand-to-sit transition, and by 17.8%MVC for the sit-to-stand transition. In the case of the RF muscle, muscle activation was noticeably reduced by 11.4%MVC during sit-to-stand, whereas no alteration was observed during stand-to-sit. Our results are comparable to studies in the current literature that investigated the effectiveness of lower limb assistive devices (Myosuit [21], JSI-KneExo [41], and E-ROWA [42]) in influencing the activation of the Vastus Lateralis/Vastus Medialis muscles among participants during the sitting and standing transitions.

As a whole, during sit-to-stand transition we were able to achieve significant reductions of muscle activity both in the

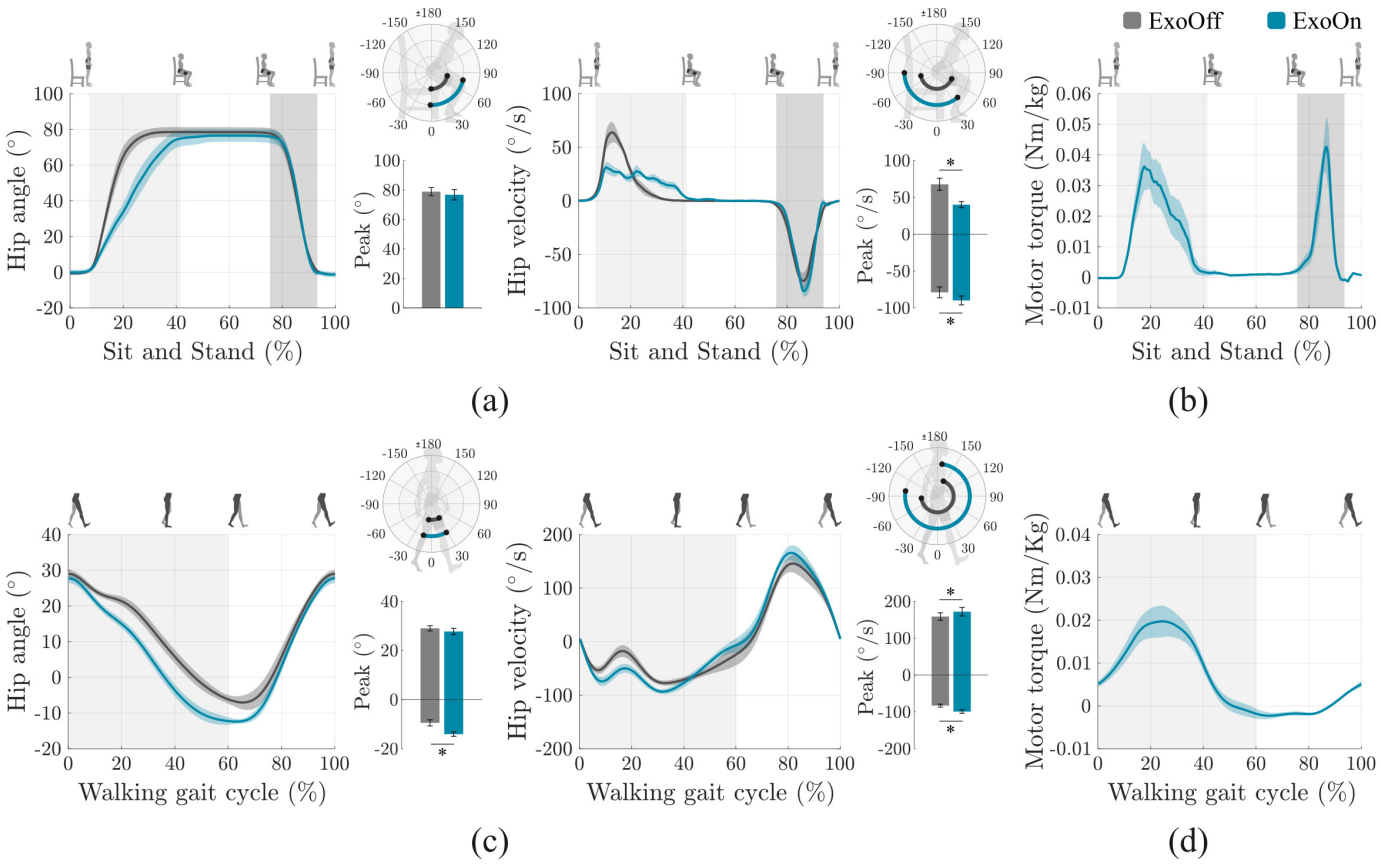

Fig. 9. **Motor torque and the influence of exosuit on users movement angle and angular velocity.** (a) Thigh angle and angular velocity profiles during sit-and-stand movements in *ExoOff* (grey) and *ExoOn* (blue) conditions. The shaded areas respectively represent the sit-to-stand process (light grey) and the stand-to-sit process (dark grey) during the sit-and-stand duration. (b) The motor torque variation during sit-and-stand transitions in *ExoOn*. (c) The thigh angle and angular velocity profiles during walking movements and the corresponding (d) motor torque. The shaded areas (light grey) illustrate the hip extension phase during walking and unshaded areas indicate the hip flexion phase during walking. The polar grids adjacent to the curves intuitively displays the range of motion of the hip joint across steps and participants during sit-and-stand and walking movements. Below them, the bars represent the positive and negative peak values for the corresponding angles and angular velocities. Asterisks * indicate statistically significant differences.

VL and RF, while during stand-to-sit, only the VL muscle significantly reduced its activation. One plausible explanation is that during the stand-to-sit transition, other lower limb muscles are physiologically more involved in facilitating the sit-down movement, rather than the RF [43]. Hence, a lack of significant decrease in RF muscle activation levels aligns with the task requirements and the absence of assistance to this muscle.

Moreover, we conducted an assessment of participants' sitting and walking energy expenditure while using the assistive system. Energy expenditure serves as a crucial indicator of the cost of a physical activity and the ability to save energy for a task correlates with increased movement efficiency [44]. Therefore, exploring methods and tools to decrease energy consumption required for movement holds great significance. The study's results revealed significant benefits of the exosuit in reducing energy consumption during continuous walking, resulting in an average 12.7% decrease in metabolic cost of transport. This suggests that using this device enables individuals to walk more efficiently, underscoring the positive impact of such assistive tools. In our study, we did not observe significant advantages of the exosuit in reducing users' energy expenditure during sitting and standing activities. However, it is important to note that the rapid nature of these movements prevents metabolic measurements from reaching a steady state, making it challenging to accurately estimate energy consumption. Moreover, the coordinated assistive forces from the exosuit during these actions: supporting while sitting and assisting while standing, could have impacted the assessment. It is possible that any potential energy savings during standing might have been offset by the resistive action from the exosuit during sitting. Yet, due to delays in the measurement of steady-state metabolic data [45], precise segmentation of these action is not feasible. For future investigations, a more comprehensive series of tests involving an increased number of sit-and-stand transitions is essential to better understand the impact of the exosuit on users' energy expenditure during such activities.

In addition to evaluating the effectiveness of the LM-Ease on participants' muscles during stand-to-sit and sit-to-stand transitions and energy expenditure during ongoing walking, we further demonstrate how the use of the device affects the user's natural movement patterns. This primarily involves whether the exosuit facilitates or impedes the overall biomechanics of users, potentially leading to the adoption of unnatural or compensatory movements that increase the risk of injury or decrease movement efficiency. In this regard, our results

suggest that the device did not induce restrictions in the inherent range of motion for sitting and standing among participants. This observation indicates that the device efficiently diminished the user's muscle activation without obstructing their typical movements. Notably, as participants transitioned from stand-to-sit, there was a conspicuous reduction in their motion velocities owing to the applied supportive forces by the exosuit, with a 40.5% reduction compared to the natural sitting velocity. This indicates that the supportive force, while alleviating muscular load during the act of sitting, also contribute to a deceleration effect, potentially enhancing the steady and safety of the sitting transitions. Conversely, during the sit-to-stand transition, the device's pulling force aided users in mitigating muscular load while increasing the movement velocity.

Although the promising results demonstrate potential advantages of the *LM-Ease* in assisting fundamental activities of daily living, such as sitting, standing, and walking, there exist limitations within this study that necessitate consideration. Firstly, the sample size of participants was small, encompassing only eight healthy participants. This limitation may constrain a comprehensive evaluation of exosuit effects and the generalizability of our findings. Future research should include diverse participant groups and broaden the evaluation to include frail individuals, thereby validating our research findings among those who stand to gain the most from this technology. Secondly, results presented here derived from short-term experimental sessions. The effects and adaptability of long-term exosuit usage remain unclear, necessitating more extensive and prolonged investigations to assess the efficacy and suitability of the exosuit in facilitating lower limb mobility. Thirdly, in this study, we were not able to analyze the muscle activity involving another major muscle engaged in sit-and-stand transitions and directly assisted by our exosuit, the Gluteus Maximus. Although we gathered muscle activity data related to the Gluteus Maximus during the experiment, the device's force application points intersected with the EMG probe location, causing significant interference with the measurements. At last, in this study, we have only performed metabolic evaluations under *ExoOff* and *ExoOn* conditions. Future works should also include a more comprehensive assessment of the effects of the device's weight on the user, encompassing a third condition without wearing the exosuit. However, from this point of view, due to the device's soft structure, light weight (2.8 kg), and its placement closer to the user's center of mass rather than the active limbs, we do not expect any significant impact on the final results. This expectation is based on a biomechanical study in the literature examining the effect of added mass on body parts [46].

In daily life, frail individuals, particularly older adults, frequently rely on aids such as canes to prevent sudden falls while sitting or to aid in standing up. The LM-Ease exosuit, as developed in this study, directly addresses these challenges by providing supportive forces during the transition from standing to sitting and counteracting the effects of gravity during the transition from sitting to standing. The implementation of this technology has the potential to significantly enhance the quality of life for frail individuals and those with mobility impairments. Real-world adoption of the LM-Ease holds promise for delivering valuable mobility benefits in everyday activities.

VII. Conclusion

In this study, we introduced the design and assessment of the LM-Ease, a textile-based lower limb assistive exosuit designed to aid users in everyday activities such as sitting, standing, and walking. Findings from experiments involving young healthy participants demonstrated that the LM-Ease effectively reduced muscle activity and decreased metabolic demand during walking. Looking ahead, technologies like the LM-Ease have the potential to be seamlessly integrated into people's lives, ultimately enhancing the overall quality of life for users.

Acknowledgment

The results presented here were obtained as part of the project HeiAge and SMART-AGE (P2019-01-003) by Carl Zeiss Foundation.

References

[1] P. M. Dall and A. Kerr, "Frequency of the sit to stand task: an observational study of free-living adults," *Applied Ergonomics*, vol. 41, no. 1, pp. 58–61, 2010.

[2] W. Jeon, J. Whitall, L. Griffin, and K. P. Westlake, "Trunk kinematics and muscle activation patterns during stand-to-sit movement and the relationship with postural stability in aging," *Gait & Posture*, vol. 86, pp. 292–298, 2021.

[3] A.-M. Georgarakis, M. Xiloyannis, P. Wolf, and R. Riener, "A textile exomuscle that assists the shoulder during functional movements for everyday life," *Nature Machine Intelligence*, vol. 4, no. 6, pp. 574–582, 2022.

[4] C. Siviy, L. M. Baker, B. T. Quinlivan, F. Porciuncula, K. Swaminathan, L. N. Awad, and C. J. Walsh, "Opportunities and challenges in the development of exoskeletons for locomotor assistance," *Nature Biomedical Engineering*, vol. 7, no. 4, pp. 456–472, 2023.

[5] Y. Zhang, R. J. Kleinmann, K. J. Nolan, and D. Zanotto, "Preliminary validation of a cable-driven powered ankle–foot orthosis with dual actuation mode," *IEEE Transactions on Medical Robotics and Bionics*, vol. 1, no. 1, pp. 30–37, 2019.

[6] C. G. Welker, T. K. Best, and R. D. Gregg, "Improving sit/stand loading symmetry and timing through unified variable impedance control of a powered knee-ankle prosthesis," *IEEE Transactions on Neural Systems and Rehabilitation Engineering*, 2023.

[7] L. N. Awad, J. Bae, K. O'donnell, S. M. De Rossi, K. Hendron, L. H. Sloot, P. Kudzia, S. Allen, K. G. Holt, T. D. Ellis *et al.*, "A soft robotic exosuit improves walking in patients after stroke," *Science Translational Medicine*, vol. 9, no. 400, p. eaai9084, 2017.

[8] M. K. Ishmael, D. Archangeli, and T. Lenzi, "Powered hip exoskeleton improves walking economy in individuals with above-knee amputation," *Nature Medicine*, vol. 27, no. 10, pp. 1783–1788, 2021.

[9] A. Rodríguez-Fernández, J. Lobo-Prat, and J. M. Font-Llagunes, "Systematic review on wearable lower-limb exoskeletons for gait training in neuromuscular impairments," *Journal of Neuroengineering and Rehabilitation*, vol. 18, no. 1, pp. 1–21, 2021.

[10] J. Moon, K. Nam, J. Ryu, Y. Kim, J. Yun, S. Yang, J. Yang, and G. Lee, "Reducing sprint time with exosuit assistance in the real world," *Science Robotics*, vol. 8, no. 82, p. eadf5611, 2023.

[11] H.-J. Lee, S. Lee, W. H. Chang, K. Seo, Y. Shim, B.-O. Choi, G.-H. Ryu, and Y.-H. Kim, "A wearable hip assist robot can improve gait function and cardiopulmonary metabolic efficiency in elderly adults," *IEEE Transactions on Neural Systems and Rehabilitation Engineering*, vol. 25, no. 9, pp. 1549–1557, 2017.

[12] T. C. Bulea and R. J. Triolo, "Design and experimental evaluation of a vertical lift walker for sit-to-stand transition assistance," 2012.

[13] M. K. Shepherd and E. J. Rouse, "Design and validation of a torque-controllable knee exoskeleton for sit-to-stand assistance," *IEEE/ASME Transactions on Mechatronics*, vol. 22, no. 4, pp. 1695–1704, 2017.

[14] Y.-A. Li, Z.-J. Chen, C. He, X.-P. Wei, N. Xia, M.-H. Gu, C.-H. Xiong, Q. Zhang, T. M. Kesar, X.-L. Huang *et al.*, "Exoskeleton-assisted sit-to-stand training improves lower-limb function through modifications of muscle synergies in subacute stroke survivors," *IEEE Transactions on Neural Systems and Rehabilitation Engineering*, 2023.

[15] M. Xiloyannis, R. Alicea, A.-M. Georgarakis, F. L. Haufe, P. Wolf, L. Masia, and R. Riener, "Soft robotic suits: state of the art, core technologies, and open challenges," *IEEE Transactions on Robotics*, vol. 38, no. 3, pp. 1343–1362, 2021.

[16] J. Park, K. Nam, J. Yun, J. Moon, J. Ryu, S. Park, S. Yang, A. Nasirzadeh, W. Nam, S. Ramadurai *et al.*, "Effect of hip abduction assistance on metabolic cost and balance during human walking," *Science Robotics*, vol. 8, no. 83, p. eade0876, 2023.

[17] X. Zhang, E. Tricomi, F. Missiroli, N. Lotti, and L. Masia, "Real-time assistive control via imu locomotion mode detection in a soft exosuit: An effective approach to enhance walking metabolic efficiency," *IEEE/ASME Transactions on Mechatronics*, vol. 29, no. 3, pp. 1797–1808, 2024.

[18] J. Kim, G. Lee, R. Heimgartner, D. Arumukhom Revi, N. Karavas, D. Nathanson, I. Galiana, A. Eckert-Erdheim, P. Murphy, D. Perry *et al.*, "Reducing the metabolic rate of walking and running with a versatile, portable exosuit," *Science*, vol. 365, no. 6454, pp. 668–672, 2019.

[19] H. Lee, S. H. Kim, and H.-S. Park, "A fully soft and passive assistive device to lower the metabolic cost of sit-to-stand," *Frontiers in Bioengineering and Biotechnology*, vol. 8, p. 966, 2020.

[20] A. L. Kulasekera, R. B. Arumathanthri, D. S. Chathuranga, T. D. Lalitharatne, and R. C. Gopura, "A low-profile vacuum actuator: Towards a sit-to-stand assist exosuit," in *2020 3rd IEEE International Conference on Soft Robotics (RoboSoft)*. IEEE, 2020, pp. 110–115.

[21] K. Schmidt, J. E. Duarte, M. Grimmer, A. Sancho-Puchades, H. Wei, C. S. Easthope, and R. Riener, "The myosuit: bi-articular anti-gravity exosuit that reduces hip extensor activity in sitting transfers," *Frontiers in Neurorobotics*, vol. 11, p. 57, 2017.

[22] D. A. Winter, *Biomechanics and motor control of human movement*. John wiley & sons, 2009.

[23] G. G. Polkowski and J. C. Clohisy, "Hip biomechanics," *Sports Medicine and Arthroscopy Review*, vol. 18, no. 2, pp. 56–62, 2010.

[24] B. Laschowski, W. McNally, A. Wong, and J. McPhee, "Computer vision and deep learning for environment-adaptive control of robotic lower-limb exoskeletons," in *2021 43rd Annual International Conference of the IEEE Engineering in Medicine & Biology Society (EMBC)*. IEEE, 2021, pp. 4631–4635.

[25] X. Liu and Q. Wang, "Real-time locomotion mode recognition and assistive torque control for unilateral knee exoskeleton on different terrains," *IEEE/ASME Transactions on Mechatronics*, vol. 25, no. 6, pp. 2722–2732, 2020.

[26] Y. Qian, Y. Wang, C. Chen, J. Xiong, Y. Leng, H. Yu, and C. Fu, "Predictive locomotion mode recognition and accurate gait phase estimation for hip exoskeleton on various terrains," *IEEE Robotics and Automation Letters*, vol. 7, no. 3, pp. 6439–6446, 2022.

[27] J. Spanias, A. Simon, S. Finucane, E. Perreault, and L. Hargrove, "Online adaptive neural control of a robotic lower limb prosthesis," *Journal of Neural Engineering*, vol. 15, no. 1, p. 016015, 2018.

[28] T. Yan, A. Parri, V. Ruiz Garate, M. Cempini, R. Ronsse, and N. Vitiello, "An oscillator-based smooth real-time estimate of gait phase for wearable robotics," *Autonomous Robots*, vol. 41, pp. 759–774, 2017.

[29] E. Tricomi, N. Lotti, F. Missiroli, X. Zhang, M. Xiloyannis, T. Müller, S. Crea, E. Papp, J. Krzywinski, N. Vitiello *et al.*, "Underactuated soft hip exosuit based on adaptive oscillators to assist human locomotion," *IEEE Robotics and Automation Letters*, vol. 7, no. 2, pp. 936–943, 2021.

[30] D. Quintero, D. J. Lambert, D. J. Villarreal, and R. D. Gregg, "Real-time continuous gait phase and speed estimation from a single sensor," in *2017 IEEE Conference on Control Technology and Applications (CCTA)*. IEEE, 2017, pp. 847–852.

[31] E. Tricomi, F. Missiroli, M. Xiloyannis, N. Lotti, X. Zhang, M. Stefanakis, M. Theisen, J. Bauer, C. Becker, and L. Masia, "Soft robotic shorts improve outdoor walking efficiency in older adults," 2024.

[32] I. Kang, D. D. Molinaro, S. Duggal, Y. Chen, P. Kunapuli, and A. J. Young, "Real-time gait phase estimation for robotic hip exoskeleton control during multimodal locomotion," *IEEE Robotics and Automation Letters*, vol. 6, no. 2, pp. 3491–3497, 2021.

[33] L. Breiman, "Random forests," *Machine Learning*, vol. 45, pp. 5–32, 2001.

[34] Z.-H. Zhou, *Machine learning*. Springer Nature, 2021.

[35] H. J. Hermens, B. Freriks, C. Disselhorst-Klug, and G. Rau, "Development of recommendations for semg sensors and sensor placement procedures," *Journal of Electromyography and Kinesiology*, vol. 10, no. 5, pp. 361–374, 2000.

[36] S. Kipp, W. C. Byrnes, and R. Kram, "Calculating metabolic energy expenditure across a wide range of exercise intensities: the equation matters," *Applied Physiology, Nutrition, and Metabolism*, vol. 43, no. 6, pp. 639–642, 2018.

[37] X. Zhang, E. Tricomi, F. Missiroli, N. Lotti, X. Ma, and L. Masia, "Improving walking assistance efficiency in real-world scenarios with soft exosuits using locomotion mode detection," in *2023 International Conference on Rehabilitation Robotics (ICORR)*. IEEE, 2023, pp. 1–6.

[38] M. Roebroeck, C. Doorenbosch, J. Harlaar, R. Jacobs, and G. Lankhorst, "Biomechanics and muscular activity during sit-to-stand transfer," *Clinical Biomechanics*, vol. 9, no. 4, pp. 235–244, 1994.

[39] X. Liu, Z. Zhou, J. Mai, and Q. Wang, "Real-time mode recognition based assistive torque control of bionic knee exoskeleton for sit-to-stand and stand-to-sit transitions," *Robotics and Autonomous Systems*, vol. 119, pp. 209–220, 2019.

[40] F. L. Haufe, A. M. Kober, P. Wolf, R. Riener, and M. Xiloyannis, "Learning to walk with a wearable robot in 880 simple steps: a pilot study on motor adaptation," *Journal of Neuroengineering and Rehabilitation*, vol. 18, pp. 1–14, 2021.

[41] L. Mišković, T. Brecelj, M. Dežman, and T. Petrič, "Design and evaluation of the jsi-kneexo: active, passive, pneumatic, portable knee exoskeleton," *arXiv preprint arXiv:2306.16000*, 2023.

[42] W. Huo, S. Mohammed, Y. Amirat, and K. Kong, "Active impedance control of a lower limb exoskeleton to assist sit-to-stand movement," in *2016 IEEE International Conference on Robotics and Automation (ICRA)*. Ieee, 2016, pp. 3530–3536.

[43] S. Ferrante, A. Pedrocchi, and G. Ferrigno, "Electromyographic analysis of standing up and sitting down," in *Proceedings of the International Functional Electrical Stimulation Society Conference*, 2005.

[44] C. J. Caspersen, K. E. Powell, and G. M. Christenson, "Physical activity, exercise, and physical fitness: definitions and distinctions for health-related research." *Public Health Reports*, vol. 100, no. 2, p. 126, 1985.

[45] J. C. Selinger and J. M. Donelan, "Estimating instantaneous energetic cost during non-steady-state gait," *Journal of Applied Physiology*, vol. 117, no. 11, pp. 1406–1415, 2014.

[46] R. C. Browning, J. R. Modica, R. Kram, and A. Goswami, "The effects of adding mass to the legs on the energetics and biomechanics of walking," *Medicine & Science in Sports & Exercise*, vol. 39, no. 3, pp. 515–525, 2007.

Xiaohui Zhang received the Ph.D. degree in computer engineering from Heidelberg University in 2024, Heidelberg, Germany, and the Master degree in control engineering from the Nanjing University of Aeronautics and Astronautics in 2019, Nanjing, China.

She is currently a PostDoc Researcher under the supervision of Prof. Lorenzo Masia in computer science with the Institute of Computer Engineering, Heidelberg University, Germany. Her research interests include human-machine interaction control strategies for wearable assistive devices, human motion intention detection.

Enrica Tricomi (Graduate Student Member, IEEE) received the bachelor's and the master's degrees in biomedical engineering from the Politecnico di Torino, Turin, Italy, in 2017 and 2019, respectively. She is now working toward the Ph.D. degree in medical engineering at Heidelberg University, Heidelberg, Germany, under the supervision of Prof. Dr. Lorenzo Masia.

Her research interests include the design and implementation of novel control strategies for wearable robotic devices to assist and augment human motor performances. She is currently serving as the Chair of the Student's Activities Committee (SAC) of the IEEE Robotics and Automation Society (RAS).

Xunju Ma is studying at the School of Mechatronical Engineering, Beijing Institute of Technology for his Ph.D. degree in Engineering.

His main research interest includes wearable exoskeleton robot, recognition and prediction of human motion intention and human-exoskeleton cooperative control.

Manuela Gomez-Correa received her bachelor's degree in Bioengineering from the University of Antioquia, Medellín, Colombia, in 2022. She is currently working toward her master's degree in computer sciences applied to biomedical engineering at the Instituto Politécnico Nacional, Mexico City, Mexico, under the supervision of Dr. Mariana Ballesteros and Dr. David Cruz-Ortiz.

Her research focuses on wearable sensors, biosignal processing, instrumentation, and mechanical design.

Alessandro Ciaramella received the bachelor's degree in mechanical engineering from the University of Pisa and the honors diploma in industrial engineering from the Sant'Anna School of Advanced Studies in 2020 and 2021, respectively. He is currently working towards the master's degree in robotics and automation engineering in the Department of Information Engineering, University of Pisa.

His research interests to date have focused on planning, optimization and decision making for autonomous robots, and mechanical design and control theory with application to wearable robotics and teleoperation.

Francesco Missiroli (Graduate Student Member, IEEE) received the bachelor's degree in biomedical engineering and the master's degree in bioengineering from the University of Padua, Padua, Italy, in 2016 and 2019, respectively. He is currently working toward the Ph.D. degree in medical engineering with a focus on wearable robotics with the Institute of Computer Engineering, Heidelberg University, Heidelberg, Germany, under the supervision of Prof. Dr. Lorenzo Masia.

His research interests include mechanical design, rehabilitation robotics, exoskeletons, and human–machine interfaces. He is currently serving as the Co-Chair of the Student's Activities Committee (SAC) of the IEEE Robotics and Automation Society (RAS) for the Robotics & Automation Magazine.

Luka Mišković received the M.S. degree in mechanical engineering, majoring in mechatronics and robotics from the University of Zagreb, in 2020. He is currently working toward a Ph.D. degree in mechanical engineering with a focus on wearable robotics with the Department of Automatics, Robotics, and Biocybernetics at Jozef Stefan Institute, Slovenia, and with the CoBoTaT laboratory. He is also a visiting Ph.D. student in the ARIES Lab, Heidelberg University, Germany.

His main research interests include design, actuation, and control of lower limb exoskeletons.

Huimin Su received the bachelor's degree in mechanical engineering from Northwestern Polytechnical University, Xi'an, China, in 2020, and the master's degree in mechanical engineering in 2022 from Korea Advanced Institute of Science and Technology, Daejeon, South Korea. He is currently working toward the Ph.D. degree in computer engineering with Heidelberg University, Heidelberg, Germany, under the supervision of Prof. Lorenzo Masia.

His research interests include wearable robotics, exoskeletons, human-robot interaction, and interfaces.

Lorenzo Masia (Senior Member, IEEE) is a Full Professor in "Intelligent Bio-Robotic Systems" and Deputy Director of the Munich Institute for Robotics and Machine Intelligence (MIRMI) at the Technical University of Munich (TUM) in Germany. He holds a Master Degree in Mechanical Engineering at Sapienza University of Rome (2003) and PhD (2007) at University of Padua (Italy) spending two years as researcher at the Massachusetts Institute of Technology and successively as serving as Team Leader at the Istituto Italiano di Tecnologia (Genoa, Italy). He was an Assistant Professor at Nanyang Technological University of Singapore, and Associate Professor of Biodesign at the University of Twente, Netherlands. From 2019 to 2024, he was a Full Professor in Heidelberg University, Germany.